

1 **The response of diazotrophs to nutrient amendment in the**
2 **South China Sea and western North Pacific**

3

4 Zuozhu Wen^{1,2}, Thomas J. Browning², Rongbo Dai¹, Wenwei Wu¹, Weiyang Li^{1,a},
5 Xiaohua Hu¹, Wenfang Lin¹, Lifang Wang¹, Xin Liu¹, Zhimian Cao¹, Haizheng Hong¹,
6 and Dalin Shi¹

7

8 ¹State Key Laboratory of Marine Environmental Science, Xiamen University, Xiamen,
9 Fujian, PR China

10 ²Marine Biogeochemistry Division, GEOMAR Helmholtz Centre for Ocean Research
11 Kiel, Germany

12

13 *Correspondence to:* Dalin Shi (dshi@xmu.edu.cn) and Haizheng Hong
14 (honghz@xmu.edu.cn)

15

16 a. Present address: Key Laboratory of Marine Ecosystem Dynamics, Second Institute of
17 Oceanography, Ministry of Natural Resources, Hangzhou, Zhejiang, PR China

18 **Abstract.** The availability of iron (Fe) and phosphorus (P) have been shown to be key
19 factors regulating rates of nitrogen fixation in the western Subtropical Pacific. However,
20 their relative importance at finer spatial scales between the northern South China Sea
21 (NSCS) and the western boundary of the North Pacific is poorly constrained.
22 Furthermore, nutrient limitation of specific diazotroph types has not yet been assessed.
23 Here we investigated these unknowns by carrying out measurements of (i) finer scale
24 spatial variabilities in N₂ fixation rates and diazotroph *nifH* gene abundances throughout
25 these regions, and (ii) conducting eight additional Fe and phosphate addition bioassay
26 experiments where both changes in N₂ fixation rates and the *nifH* gene abundances of
27 specific diazotrophs were measured. Overall, nitrogen fixation rates and *nifH* gene
28 abundances were lower in the NSCS than around the Luzon Strait and the western North
29 Pacific. The nutrient addition bioassay experiments demonstrated that N₂ fixation rates in
30 the central NSCS were co-limited by Fe and P, whereas in the western boundary of the
31 North Pacific they were P-limited. Changes in the abundances of *nifH* in response to
32 nutrient addition varied in how well they correlated with changes in N₂ fixation rates, and
33 in 6 out of 8 experiments the largest responses in *nifH* gene abundances were dominated
34 by either *Trichodesmium* or UCYN-B. In general, nutrient addition had a relatively
35 restricted impact on the composition of the six phylotypes that we surveyed apart from on
36 UCYN-B. This unicellular cyanobacterium group showed increased contribution to the
37 total *nifH* gene abundance following P addition at sites where N₂ fixation rates were P-

38 limited. Our study provides comprehensive evidence of nutrient controls on N₂ fixation
39 biogeography in the margin of the western North Pacific. Future research that more
40 accurately constrains nutrient supply rates to this region would be beneficial for resolving
41 what controls diazotroph community structure.

42 **1 Introduction**

43 Nitrogen fixation by diazotrophic bacteria converts abundant dinitrogen (N₂) gas into
44 ammonia, providing nearly half of the ocean's bioavailable nitrogen (N) (Gruber and
45 Galloway, 2008), which goes on to support >30% of carbon export from surface to deep
46 waters in the N-limited ocean (Böttjer et al., 2016; Wang et al., 2019). A diverse
47 community of diazotrophs has been described across the oligotrophic ocean that includes
48 *Trichodesmium*, unicellular cyanobacteria (UCYN-A and *Crocospaera*, also referred to
49 as UCYN-B), the heterocystous symbiont *Richelia* associated with diatoms (DDAs,
50 diatom-diazotroph associations), and noncyanobacterial diazotrophs (NCDs,
51 heterotrophic or photoheterotrophic bacteria) (Zehr and Capone, 2020). However, there is
52 still a lack of knowledge on what controls diazotrophic distribution, activity and
53 community structure in the current ocean.

54

55 Iron (Fe) and phosphorus (P) are believed to be key factors controlling the biogeographic
56 distribution of marine N₂ fixation (Sohm et al., 2011; Zehr and Capone, 2020; Wen et al.,
57 2022). Fe is particularly important for N₂ fixers as a cofactor for the FeS-rich
58 nitrogenase enzyme (Berman-Frank et al., 2001), whereas P is also required for genetic
59 information storage, cellular structure and energy generation. A number of nutrient-
60 addition bioassay experiments conducted in the field have shown that N₂ fixation in the
61 oligotrophic oceans can be limited by Fe or P, or co-limited by both nutrients at the same

62 time (Mills et al., 2004; Needoba et al., 2007; Grabowski et al., 2008; Watkins-Brandt et
63 al., 2011; Langlois et al., 2012; Turk-Kubo et al., 2012; Dekaezemacker et al., 2013;
64 Krupke et al., 2015; Tanita et al., 2021; Wen et al., 2022). However, few studies have
65 quantified how the supply of Fe and/or P impacts the abundance of individual
66 diazotrophic phylotypes and their community structure (Langlois et al., 2012; Moisander
67 et al., 2012; Turk-Kubo et al., 2012). Experiments conducted so far that investigated this
68 were located in the South Pacific and North Atlantic, and found diverse responses among
69 diazotrophic phylotypes to the addition of Fe and/or P. Furthermore, the responses of total
70 diazotroph abundances assessed from *nifH* gene quantifications did not qualitatively
71 match the responses of bulk N₂ fixation rates (Langlois et al., 2012; Moisander et al.,
72 2012; Turk-Kubo et al., 2012). Resolution of the specific types of diazotrophs responding
73 to nutrient supply, in addition to overall N₂ fixation rates, is potentially crucial for
74 understanding their biogeography, which in turn could be important for biogeochemical
75 function. For example, the presence of large *Trichodesmium* filaments is expected to have
76 a different fate in the microbial food web and contribute differently to the sinking flux of
77 carbon than that of small unicellular species (Bonnet et al., 2016).

78

79 The northern South China Sea (NSCS) and the neighboring western boundary of the
80 North Pacific are interacting water bodies, with the major western boundary Kuroshio
81 Current intruding into the NSCS across the Luzon Strait, generating frontal zones with

82 unique physical and biogeochemical characteristics (Du et al., 2013; Guo et al., 2017; Xu
83 et al., 2018; Huang et al., 2019; Lu et al., 2019; Li et al., 2021). Common to the full
84 regime, however, is surface waters that are warm, stratified and N-depleted, but subject to
85 elevated dust input from the Gobi Desert (Duce et al., 1991; Jickells et al., 2005). These
86 conditions potentially provide an ideal habitat for diazotrophs (Chen et al., 2003; Wu et
87 al., 2003). Investigations in these regions have shown high variability in diazotroph
88 abundances and N₂ fixation rates (Chen et al., 2003; Chen et al., 2008; Chen et al.,
89 2014; Wu et al., 2018; Lu et al., 2019), which overall increased from the NSCS basin to
90 the western boundary of the North Pacific (Wen et al., 2022). Along this gradient in N₂
91 fixation, the dominant diazotroph types switched from *Trichodesmium* in the NSCS to
92 UCYN-B in the western boundary of the North Pacific (Wen et al., 2022). Several studies
93 have hypothesized that these gradients of diazotroph abundances and N₂ fixation rates
94 were regulated by nutrient availability (specifically, Fe, P and N; Wu et al., 2003; Chen et
95 al., 2003; Chen et al., 2008; Shiozaki et al., 2014a; Shiozaki et al., 2015a). More recent
96 observational and experimental evidence supported the hypothesis that Fe:N supply ratios
97 are the main drivers of the abundance of diazotrophs and N₂ fixation rates across the
98 western North Pacific (Wen et al., 2022). With an increasing supply ratio of Fe:N from
99 the North Equatorial Current (NEC) to the Philippines Sea, Wen et al. (2022) found that
100 diazotroph abundances and N₂ fixation rates increased, and bioassay experiments
101 demonstrated evidence for N₂ fixation rates switching from Fe to P limitation or to

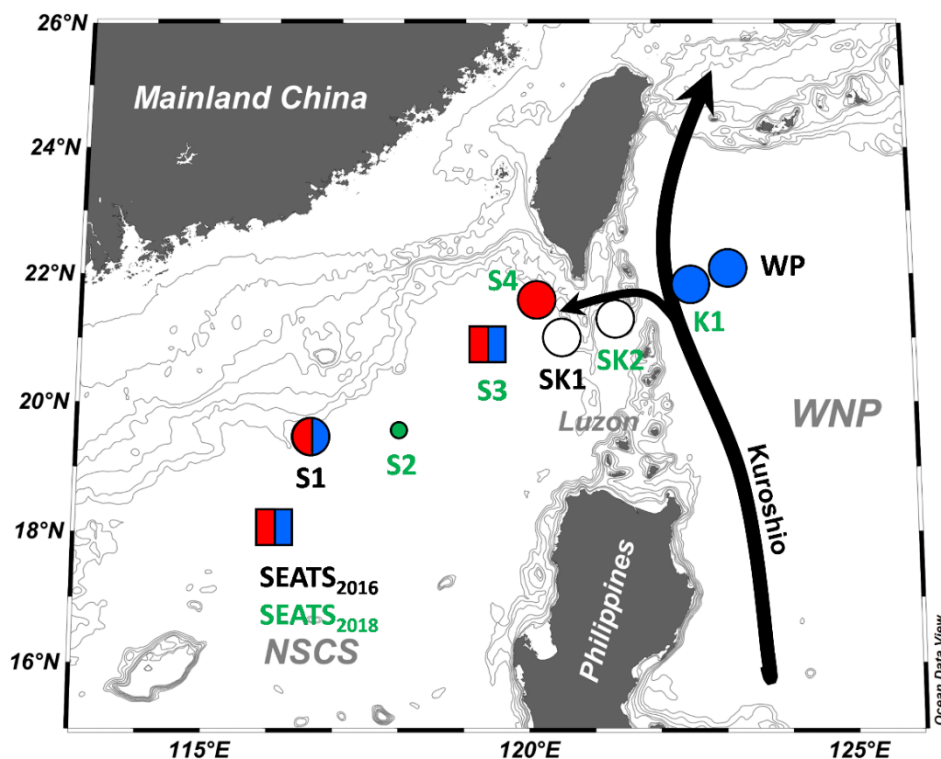
102 nutrient-replete conditions. In the NSCS, Wen et al. (2022) found N₂ fixation rates fell in
103 between NEC and Kuroshio values and bioassay experiments demonstrated rates were
104 co-limited by Fe and P, which they hypothesized was due to intermediate Fe:N supply
105 ratios (Wen et al., 2022).

106

107 Although this previous study has outlined the broad spatial pattern of nutrient regulation
108 of marine N₂ fixation throughout the western subtropical Pacific (Wen et al., 2022),
109 important questions remain. Two specific examples are: (i) the Kuroshio intrusion
110 generates a frontal zone with a unique diazotrophy regime in the NSCS (Lu et al., 2019),
111 and thus the relatively lower spatial resolution of the experiments in Wen et al. (2022)
112 and other studies (Shiozaki et al., 2014b; Chen et al., 2019) remains insufficient to
113 delineate Fe and P controls at finer spatial scales between the neighboring NSCS and the
114 western boundary of the North Pacific; and (ii) in addition to controls on N₂ fixation
115 rates, broad-scale differences in the types of diazotrophs dominating the N₂ fixer
116 community were not concretely associated with environmental drivers in experimental
117 tests for nutrient limitation, because changes in type-specific diazotroph abundances
118 following nutrient addition were not measured (Shiozaki et al., 2014b; Chen et al., 2019;
119 Wen et al., 2022). Therefore, in the present study we extend the findings of Wen et al.
120 (2022) and others by carrying out additional, higher-spatial resolution observations of
121 volumetric N₂ fixation rates and measurements of the *nifH* gene abundances of key

122 diazotrophic phylotypes from the NSCS basin to the western boundary of the North
123 Pacific (including the upstream Kuroshio) between 2016 and 2018 (Fig. 1). These new
124 observations were supplemented by a further additional eight, high volume (10 L)
125 nutrient amendment bioassay experiments throughout the transect to directly test the
126 response of both (i) N_2 fixation rates, and (ii) *nifH* gene abundances to supply of
127 potentially limiting nutrients (Fe, P, and Fe+P).

128



129

130

131 **Figure 1.** Sampling and nutrient amendment experiment locations in the northern South
132 China Sea and the western boundary of the North Pacific. One station (SEATS₂₀₁₆) was
133 sampled in 2016, three (S1, SK1, WP) were in 2017, and six (stations with green labels)
134 were in 2018. Nutrient amendment experiments were conducted at 8 of 10 stations.
135 Symbols summarize the nutrient limitation of N_2 fixation rates found at each site: red, Fe
136 limitation; blue, P limitation; split red/blue, Fe-P co-limitation; white, nutrient replete.

137 Co-limitation type is indicated by symbol type (square, independent co-limitation; circle,
138 simultaneous co-limitation). WNP, the western North Pacific. Black arrows indicate
139 Kuroshio Current and its branch.

140

141 **2 Method**

142 **2.1 Sample collection**

143 Investigations and bioassay experiments were conducted on three cruises to the NSCS
144 (stations SETAS and S1 to S4), the Luzon Strait (stations SK1 and SK2), the upstream
145 Kuroshio (station K1), and the western boundary of the North Pacific (station WP) (Fig.
146 1), between May 2016 and June 2018 onboard the R/V *Dongfanghong 2* and R/V *Tan*
147 *Kah Kee*. At each station (except station SK2 where no hydrological data are available),
148 temperature and salinity were recorded by a Seabird 911 CTD. Water samples were
149 collected using Niskin-X bottles at five or six depths (except SK2, only surface waters
150 were sampled) throughout the upper 150 m for the determination of N₂ fixation and
151 primary production rates. Seawaters from each depth were also sampled for the analysis
152 of *nifH* gene abundance. Samples for nutrient analysis were also collected. Seawater for
153 the bioassay experiments (at 8 of 10 stations) was collected using a trace-metal-clean
154 towed sampling device located around 2-5 m depth with suction provided by a Teflon
155 bellows pump. Seawaters were sampled in a dedicated trace-metal-clean laminar flow
156 hood maintained over-pressurized by HEPA-filtered air. During the cruise in 2018
157 (stations with green labels in Fig. 1), surface waters were sampled under trace-metal-

158 clean conditions for the determination of total particulate Fe concentration.

159

160 **2.2 N₂ fixation and primary production rate measurements**

161 N₂ fixation rates were determined by the ¹⁵N₂ gas dissolution method (Mohr et al., 2010),
162 combined with a primary production assay using NaH¹³CO₃ (99 atom% ¹³C, Cambridge
163 Isotope Laboratories). Briefly, 0.22 μm-filtered surface seawater was degassed using a
164 Sterapore membrane unit (20M1500A: Mitsubishi Rayon Co., Ltd., Tokyo, Japan) as
165 described in Shiozaki et al. (2015b). After that, 20 mL 98.9 atom% pure ¹⁵N₂ gas
166 (Cambridge Isotope Laboratories) was injected into a gas-tight plastic bag (Tedlar®PVF,
167 Dalian Delin Gas Packing Co., Ltd) containing 2 L of the degassed seawater and allowed
168 to fully equilibrate before use. The N₂ fixation and primary production incubations were
169 conducted in duplicate 4.3 L Nalgene polycarbonate bottles. Samples were spiked with
170 100 mL ¹⁵N₂ enriched filtered seawater from the same site and incubated on-deck for 24
171 h. The final ¹⁵N₂ enriched seawater concentration in the incubation bottles was not
172 measured directly during this study. We thus employed a ¹⁵N₂ atom% of 1.40 ± 0.08
173 atom% (ranges from 1.28 to 1.56 atom%, $n = 17$) measured in a following cruise in 2020
174 (Wen et al., 2022), during which the N₂ fixation incubations were conducted using the
175 same approach, reagents, and equipment as for the study described here. For primary
176 production measurements, NaH¹³CO₃ solution was added to a final amended
177 concentration of 100 μM. After that, the bottles were covered with a neutral-density

178 screen to adjust the light to the levels at sampling depths, and then were incubated for 24
179 h in an on-deck incubator continuously flushed with surface seawater. Incubated samples
180 were filtered onto pre-combusted (450 °C, 4 h) GF/F filters, and the particulate organic
181 matter from each depth were also collected to determine background POC/PON
182 concentrations and their natural $^{13}\text{C}/^{15}\text{N}$ abundances.

183

184 All filter samples were acid fumed to remove the inorganic carbon and then analyzed
185 using an elemental analyzer coupled to a mass spectrometer (EA-IRMS, Thermo Fisher
186 Flash HT 2000-Delta V plus). The N_2 fixation and primary production rates were then
187 calculated according to Montoya et al. (1996) and Hama et al. (1983), respectively. The
188 detection limits of N_2 fixation rates were then calculated according to Montoya et al.
189 (1996), taking 4‰ as the minimum acceptable change in the $\delta^{15}\text{N}$ of particulate nitrogen.

190 All parameters involved in N_2 fixation rate calculation are shown in Supplementary
191 Materials. To represent the inventories, the upper 150 m depth-integrated N_2 fixation rate
192 and primary production were calculated by the trapezoidal integration method.

193

194 **2.3 *nifH* gene abundance**

195 At each depth, 4.3 L seawater samples for DNA extraction were filtered onto 0.22 μm
196 pore-sized membrane filters (Supor200, Pall Gelman, NY, USA) and then frozen in liquid
197 N_2 . To extract the DNA, membranes were cut into pieces under sterile conditions, and

198 then extracted using the QIAamp[®] DNA Mini Kit (Qiagen) following the manufacturer's
199 protocol. The quantitative polymerase chain reaction (qPCR) analysis was targeted on the
200 *nifH* phylotypes of *Trichodesmium* spp., unicellular cyanobacterial UCYN-A1, UCYN-
201 A2, and UCYN-B, *Richelia* spp. (het-1), and a gamma-proteobacterium (γ -24774A11),
202 using previously designed primers and probe sets (Supplementary Table S1; Church et al.,
203 2005a; Church et al., 2005b; Moisander et al., 2008; Thompson et al., 2014). A recent
204 study suggested that the primers for UCYN-A2 also target UCYN-A3 and thus cannot be
205 used to differentiate between these two phylotypes (Farnelid et al., 2016). Therefore, we
206 used the convention UCYN-A2/A3 when referring to these two groups. The *nifH*
207 standards were obtained by cloning the environmental sequences from previous samples
208 collected from the SCS. qPCR analysis was carried out as described previously (Church
209 et al., 2005a) with slight modifications. Triplicate qPCR reactions were run for each
210 environmental DNA sample and for each standard on a CFX96 Real-Time System (Bio-
211 Rad Laboratories). Standards corresponding to between 10^1 and 10^7 copies per well were
212 amplified in the same 96-well plate. The amplification efficiencies of PCR were always
213 between 90-105%, with R^2 values > 0.99 . The quantification limit of the qPCR reactions
214 was 10 *nifH* gene copies per reaction, and 1 μ L from 100 or 150 μ L template DNA was
215 applied to qPCR assay, which was equivalent to approximately ~230-350 gene copies per
216 L of seawater sample filtered (4.3 L).

217

218 A previous study has reported that *nifH* gene polyploidy exists in *Trichodesmium*
219 (Sargent et al., 2016), which may impact the estimates of diazotroph compositions.
220 However, given that the degree of polyploidy can vary significantly (ranging from 1 to
221 1405; Sargent et al., 2016; White et al., 2018), with a potential dependence on the growth
222 conditions, nutrient status, developmental stage, and cell cycle (see references in
223 Karlusich et al., 2021), we did not attempt to account/correct for this in calculations of
224 proportions of the different diazotrophs.

225

226 **2.4 Bioassay experiments**

227 Acid-cleaned Nalgene polycarbonate carboys (10 L) were filled with near surface
228 seawater from the towed fish system. Trace metal clean techniques were strictly applied
229 in experimental setup and manipulations. All materials including the degas unit and
230 Tedlar[®]PVF bags that came in contact with the incubation water were acid-washed in a
231 Class-100 cleanroom before use. Nutrient amendments at all sites were Fe, P, and Fe+P.
232 Surface dissolved Fe and P concentrations previously reported in the NSCS were 0.17-
233 1.01 nM and 5-20 nM respectively (Wu et al., 2003; Zhang et al., 2019). In order to
234 obtain a measurable response within the relatively short 72-hour experimental period, 2
235 nM Fe and 100 nM P (chelexed and filter-sterilized) were added to each of the treatment
236 bottles. Control bottles incubated with no nutrient treatment were included in all
237 experiments. Treatments for 7 out of 8 experiments were conducted with 3 replicates.

238 However, there were three cases when one of the triplicate samples was lost due to
239 filtration errors (one +Fe+P carboy at station S1, one NFR/PP sample of +Fe+P at station
240 WP, and one NFR/PP sample of +P sample at station S3). In addition, for the bioassay
241 experiment at station SEATS₂₀₁₆, sufficient water was only available to conduct the
242 experiment with 2 replicates for control and +Fe+P treatments, while +Fe and +P retained
243 3 replicates. All carboys were then incubated for 3 days in a screened on-deck incubator
244 (a ~400-L clear on-deck incubator with inflow and outflow) continuously flushed with
245 surface seawater. After 72 hours pre-incubation, subsamples were collected for the
246 determination of Chl *a* concentration, N₂ fixation rate and *nifH* gene abundance. ¹⁵N₂
247 enriched seawater was prepared as described above, except that all the materials coming
248 in contact with the seawater were acid-cleaned before use.

249

250 **2.5 Macronutrient and chlorophyll *a* analyses**

251 Samples for macronutrient analyses were collected in 125-mL acid-washed high-density
252 polyethylene (HDPE) bottles (Nalgene), and analyzed onboard using a Four-channel
253 Continuous Flow Technicon AA3 Auto-Analyzer (Bran-Lube GmbH). The detection
254 limits for NO₃⁻+NO₂⁻ and PO₄³⁻ were 0.1 μmol L⁻¹ and 0.08 μmol L⁻¹, respectively. The
255 nitracline was defined as the depth at which NO_x concentration equaled 0.1 μmol L⁻¹ (Le
256 Borgne et al., 2002). Surface seawaters were additionally sampled for the measurement of
257 low-level nutrient concentrations in the 2018 cruise and NO₃⁻+NO₂⁻ was determined

258 following Zhang (2000) whilst PO_4^{3-} was analyzed following Ma et al., (2008). Samples
259 for chlorophyll *a* analysis were collected on nominal 0.7 μm pore-size GF/F filters
260 (Whatman), extracted in 90% acetone, and analyzed fluorometrically on a Turner Designs
261 fluorometer (Welschmeyer 1994).

262

263 **2.6 Particulate Fe concentration**

264 Total particulate Fe ($\text{PFe}_{\text{total}}$) and intracellular Fe ($\text{PFe}_{\text{intra}}$) were sampled under laminar
265 flow hood. Briefly, 4-9 L of surface waters were filtered onto acid-cleaned 0.22- μm
266 polycarbonate membrane filters. For $\text{PFe}_{\text{intra}}$ samples, in order to remove metal bound to
267 the cell surface, cells were exposed twice to an oxalate-EDTA solution for 5 minutes and
268 rinsed nine times with Chelex-cleaned 0.56 mol L^{-1} NaCl solution (Li et al., 2020).

269 $\text{PFe}_{\text{total}}$ and $\text{PFe}_{\text{intra}}$ concentrations were then determined by ICP-MS (ICP-MS 7700X,
270 Agilent).

271

272 **2.7 Statistical analysis**

273 Significance of differences among nutrient treatments of bioassay experiments (for N_2
274 fixation rate) were tested by ANOVA followed by Fisher PSLD test, using R-4.1.2.

275 Pairwise correlation between N_2 fixation rates, diazotroph groups and environmental
276 factors was analyzed using Pearson correlation. A significance level of $p < 0.05$ was

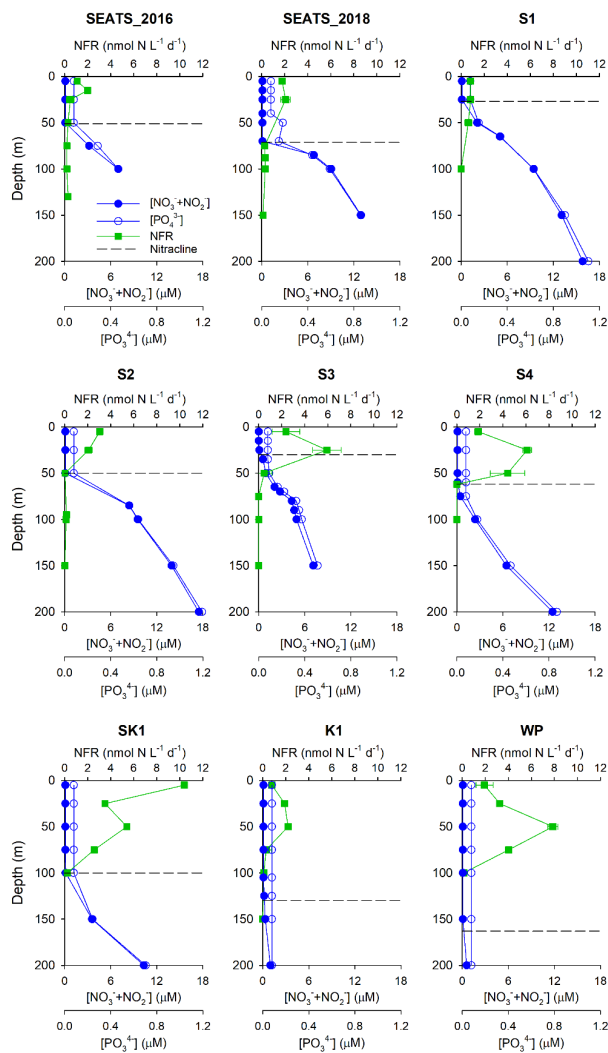
277 applied, except as noted where significance was even greater. It should be noted that

278 those statistical results that were produced from only two replicates are not strictly
 279 statistically valid, but for completeness the posthoc test results are nevertheless still
 280 included here.

281

282 3 Results

283 3.1 Spatial variations of N₂ fixation rates and diazotroph composition



284

285

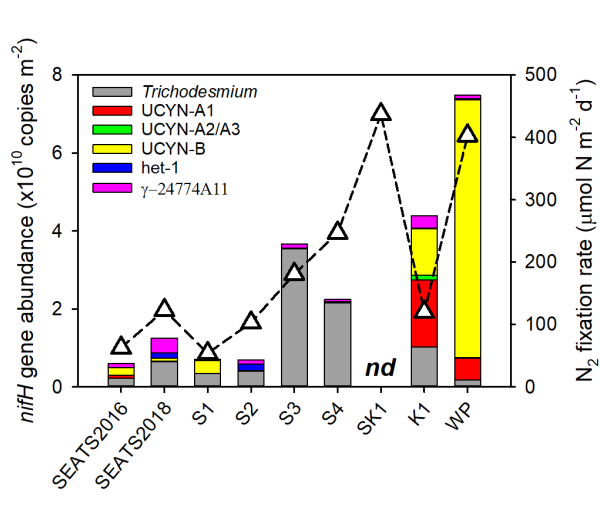
286 **Figure 2.** Vertical profiles of N₂ fixation rates. Green squares, N₂ fixation rate (NFR,

287 nmol N L⁻¹ d⁻¹); blue solid circles, NO₃⁻+NO₂⁻ concentrations (μM); blue open circles,
 288 PO₄³⁻ concentrations (μM). The dashed line indicates the nitracline depth. Note that no
 289 profile data were available at station SK2.

290

291 Our survey revealed substantial spatial variability in N₂ fixation rates and *nifH* gene
 292 abundances across the study area (Figs. 2 and 3). Vertically, high N₂ fixation rates were
 293 found in the upper 50 m (ranged from below detection limit to 10.4 ± 0.01 nmol N L⁻¹ d⁻¹
 294 ¹), rates dropped rapidly at greater depths (Fig. 2), and surface rates were positively
 295 correlated with depth-integrated rates (Pearson $r = 0.68$, $p = 0.043$, Supplementary Table
 296 S2). Horizontally, depth-integrated N₂ fixation rates were generally low at the central
 297 NSCS basin stations (SEATS, S1 and S2, on average 86 ± 33 μmol N m⁻² d⁻¹), elevated at
 298 stations close to the western edge of the Luzon Strait (S3 and S4, on average 214 ± 47
 299 μmol N m⁻² d⁻¹), and were highest at the Luzon Strait station (SK1, 437 μmol N m⁻² d⁻¹)
 300 and the western North Pacific boundary station (WP, 403 μmol N m⁻² d⁻¹) (Figs. 1, 3 and
 301 Table 1).

302



303

304 **Figure 3.** Depth-integrated (upper 150 m) *nifH* gene abundances (bars) and N₂ fixation
305 rates (triangles). Note that depth-integrated N₂ fixation rates and *nifH* gene abundances
306 were not available at station SK2. nd, not determined.

307

308 **Table 1.** Environmental conditions, N₂ fixation, and primary production rates. Sea
309 surface temperature (SST) and salinity (SSS), chlorophyll *a* concentration, surface
310 dissolved inorganic nitrogen (SDIN) and phosphorus (SDIP), nitracline depth (D_{Nitr}),
311 surface N₂ fixation rate (SNF), upper 150 m depth-integrated N₂ fixation rate (INF) and
312 primary production (IPP) at each station. nd, not determined.

Station	SST (°C)	SSS	Chl <i>a</i> (µg/L)	SDIN (nM)	SDIP (nM)	D _{Nitr} (m)	SNF	INF	IPP
							(nmol N L ⁻¹ d ⁻¹)	(µmol N m ⁻² d ⁻¹)	(mmol C m ⁻² d ⁻¹)
SEATS ₂₀₁₆	30.3	33.46	0.26	nd	nd	51	1.1	63	44
SEATS ₂₀₁₈	30.3	33.46	0.11	9.5	16.8	71	1.8	123	24
S1	29.5	33.73	0.24	nd	nd	27	0.8	54	43
S2	29.4	33.75	0.10	9.6	13.0	50	3.0	103	24
S3	28.7	33.53	0.15	11.1	16.2	30	2.4	181	98
S4	29.5	33.74	0.17	5.1	11.7	62	1.8	247	59
SK1	30.5	33.62	0.22	nd	nd	100	10.4	437	11
SK2	nd	nd	0.11	nd	nd	nd	2.0	nd	nd
K1	29.1	34.45	0.11	5.9	16.8	130	0.8	120	19
WP	30.9	34.47	0.11	nd	nd	163	1.9	403	9

313

314 A significant positive correlation was found between the depth-integrated *nifH* gene
315 abundance and N₂ fixation rate (Pearson $r = 0.72$, $p = 0.046$, Supplementary Table S2),
316 demonstrating that the *nifH* gene abundances of these major diazotroph phylotypes that
317 we surveyed well explained the major variability in measured rates. However,
318 considerable spatial variation was found in the specific diazotrophs supporting N₂

319 fixation (Fig. 3). *Trichodesmium* dominated the total *nifH* gene abundance throughout the
320 water column of the NSCS (52-96% of the total *nifH* gene abundance, excluding station
321 SEATE₂₀₁₆). In contrast, at the Kuroshio station K1, unicellular diazotrophic
322 cyanobacteria (UCYN-A and UCYN-B) were the most abundant *nifH* gene phylotypes,
323 and at station WP, UCYN-B alone was dominant (Fig. 3 and Supplementary Table S3). It
324 should be noted that *nifH* gene polyploidy exists in *Trichodesmium* (Sargent et al., 2016),
325 which may have an important impact on the estimates of both in situ and nutrient-treated
326 diazotroph compositions (see Method).

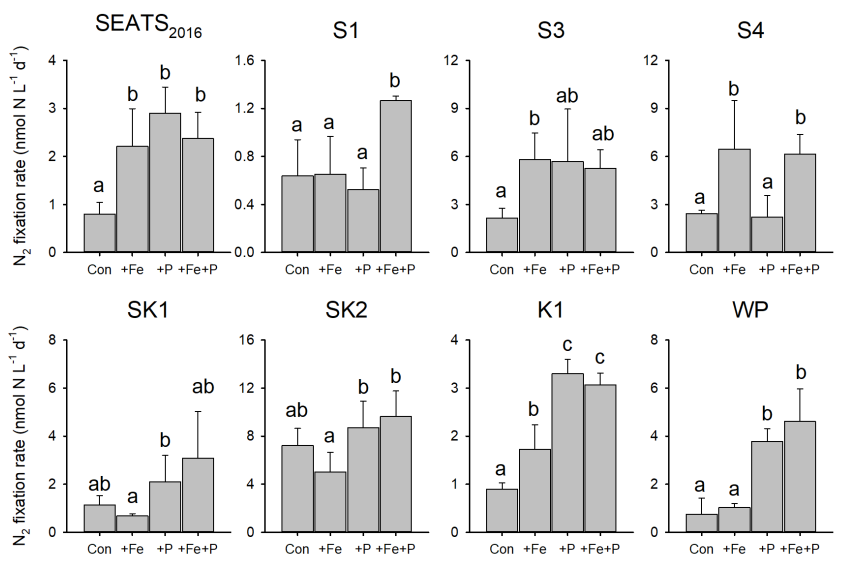
327

328 **3.2 Diazotroph response to Fe and P supply**

329 To directly test which nutrients were limiting overall N₂ fixation rates and the *nifH* gene
330 abundances of individual diazotrophs, we conducted eight, ~3-day nutrient addition
331 bioassay experiments (Figs. 4 and 5). The responses of N₂ fixation rate to different
332 combinations of Fe and P supply demonstrated a coherent geographic switch across the
333 study area (Figs. 1, 4 and 5). At stations towards to the NSCS basin (SEATS₂₀₁₆, S1 and
334 S3), N₂ fixation rates were co-limited by Fe and P. Two forms of this co-limitation were
335 identified: (i) only simultaneous Fe and P addition stimulated N₂ fixation rates
336 ('simultaneous co-limitation', station S1, Fig. 4); (ii) independent addition of either Fe or
337 P alone, or supply of Fe and P in combination, enhanced N₂ fixation rates ('independent
338 co-limitation', station SEATS₂₀₁₆, Fig 4). For the experiment conducted at station S3, in

339 which N₂ fixation was also recognized to be independently co-limited, the rates in all
 340 nutrient-amended groups increased by 1.44-1.70 times compared to control values,
 341 although statistical significances were not observed in +P and +Fe+P treatments (Fig. 4).
 342 Further to the northeast, in contrast, N₂ fixation rates were only stimulated by nutrient
 343 combinations containing Fe at S4 and by combinations containing P at K1 and WP,
 344 suggesting single limitation by Fe or P, respectively, at these sites (Fig. 4). Although Fe
 345 addition also appeared to stimulate N₂ fixation rates at station K1, P was generally the
 346 major limiting nutrient at this station taking into account the responses of both N₂ fixation
 347 rates and *nifH* gene abundance (see below) (Figs. 4 and 5). At stations SK1 and SK2 in
 348 the Luzon Strait, mean N₂ fixation rates and *nifH* gene abundances were not significantly
 349 affected by nutrient amendments, suggesting that both Fe and P availability were not
 350 limiting N₂ fixation rates (Figs. 4 and 5).

351



352

353

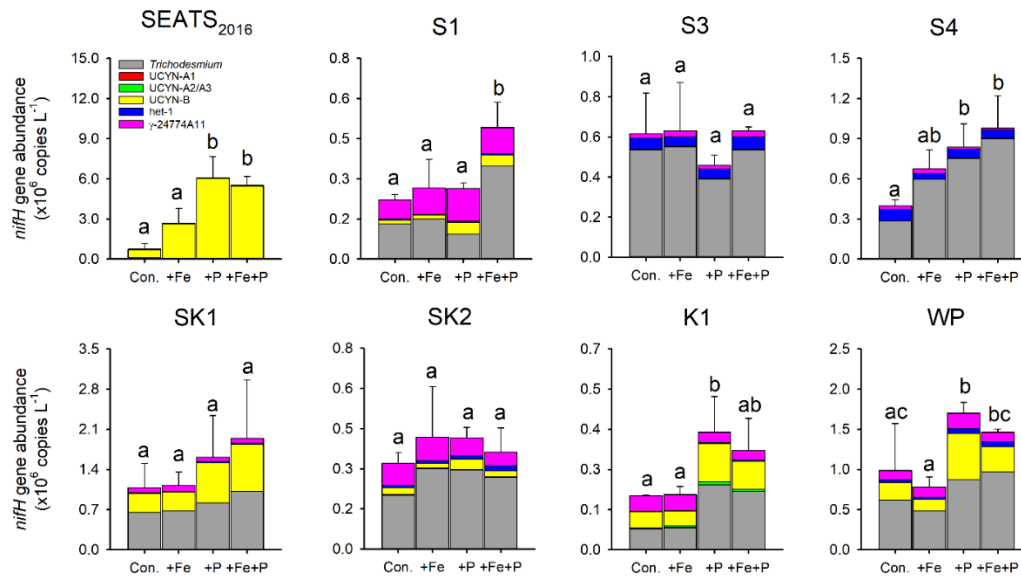
354 **Figure 4.** Response of N₂ fixation to nutrient amendment. Error bars represent the
355 standard deviation of biological replicates ($n = 2$ or 3). Different letters above error bars
356 indicate statistically significant differences ($p < 0.05$) between treatments (ANOVA
357 followed by Fisher PLSD test). Note that statistical results were produced from only two
358 replicates for control and +Fe+P at station SEATS₂₀₁₆, +Fe+P at stations S1 and WP, and
359 +P at station S3, and should thus be treated with caution.

360

361 Further detail as to the drivers of the N₂ fixation responses to Fe and P additions was
362 provided by the species-level analysis of diazotroph *nifH* from the treatment bottles. In
363 general, responses of total *nifH* gene abundance to Fe and P amendments were
364 qualitatively consistent with N₂ fixation rates at most sites, that is, the nutrient(s) limiting
365 N₂ fixation rates also limited the diazotroph *nifH* abundance (Figs. 4 and 5). The
366 exceptions were at stations S3 and S4, where variability in *nifH* abundances was observed
367 in response to nutrient treatment (station S3) or overall trends differed between *nifH*
368 abundances and N₂ fixation rates (station S4; enhanced *nifH* abundance in response to +P,
369 whereas rates only responded to +Fe). Quantitatively, the responses of N₂ fixation rates
370 and *nifH* biomass to nutrient addition were not well correlated (total *nifH* abundance
371 increase rate, calculated as $\text{Ln}(nifH_{\text{treatment}}/nifH_{\text{control}})/\text{incubation time}$, versus the
372 N₂ fixation increase rate following nutrient supply, $R^2 = 0.07$, $p = 0.21$; Supplementary
373 Fig. S1), despite initial background *nifH* abundances and N₂ fixation rates being well
374 correlated (Pearson $r = 0.72$, $p = 0.046$, Supplementary Table S1). This suggested a
375 decoupling of the rates of change in biomass and N₂ fixation rates following nutrient

376 addition over the relative short incubation timescales (~3 days).

377



378

379

380 **Figure 5.** Response of diazotroph phylotypes to nutrient amendment. Bar heights
381 represent the mean total *nifH* concentration and error bars the standard deviation of
382 biological replicates ($n = 2$ or 3). Different letters above error bars indicate a statistically
383 significant difference ($p < 0.05$) between treatments (ANOVA followed by Fisher PLSD
384 test). Note that statistical results were produced from only two replicates for control and
385 +Fe+P at station SEATS₂₀₁₆, control and +Fe+P at station S1, and +P and +Fe+P at station
386 SK2, and should thus be treated with caution.

387

388 Overall, the composition of the six diazotroph phylotypes that we surveyed were not

389 greatly changed after nutrient amendments (Fig. 5). *Trichodesmium* and UCYN-B were

390 the two most dominant *nifH* phylotypes in all experimental waters that contributed to the

391 enhanced total *nifH* gene abundance after nutrient additions (Figs. 3, 5 and

392 Supplementary Fig. S1). Despite showing independent co-limitation in response to Fe and

393 P supply at station SEATS₂₀₁₆ (Fig. 4), as reflected by equally responding N_2 fixation

394 rates, UCYN-B, the dominant *nifH* phylotype in non-amended control waters, increased
395 2-fold more following P addition in comparison to Fe addition (Fig. 5 and Supplementary
396 Fig. S2). Furthermore, no significant changes in *nifH* were observed at station S3, where
397 N₂ fixation rates were also independently Fe-P co-limited. More consistent between the
398 N₂ fixation rates and *nifH* biomass changes were the *nifH* responses at station S1, with
399 overall *nifH* concentrations only responding to Fe+P additions, matching the N₂ fixation
400 response. This was mostly driven by co-limitation of *Trichodesmium*, whereas UCYN-B
401 responded only to P supply (Fig. 5 and Supplementary Fig. S2).

402

403 In contrast to the Fe limitation of N₂ fixation rates found at station S4, *nifH* abundances
404 showed the most significant responses to the combined supply of Fe and P. However, at
405 sites where N₂ fixation rates were P-limited (K1 and WP) overall *nifH* concentrations also
406 responded most to P addition, with contributions from both *Trichodesmium* and UCYN-B
407 (Fig. 5). In addition, *het-1* also increased significantly with +P combinations at stations
408 K1 and WP (Supplementary Fig. S2). By contrast, γ -24774A11, which also accounted for
409 a substantial fraction of the total *nifH* gene abundance (up to 31%), did not show clear
410 enhancement to nutrient additions (Supplementary Fig. S2), suggesting that it was not Fe-
411 and/or P-limited. Interestingly, UCYN-A disappeared in the nutrient amendment
412 experiments, although they were abundant in the initial water at stations K1 and WP
413 (Figs. 3 and 5), possibly due to an unconstrained bottle effect (Göran et al., 2003).

414

415 **4 Discussion**

416 In the present study, surface dissolved inorganic nitrogen (DIN) and phosphorus (DIP)
417 concentrations in our study area were depleted (5.1-11.1 nM DIN, 11.7-16.8 nM DIP,
418 Table 1). Furthermore, bioassay incubations shown no significant responses of Chl *a*
419 concentration to the amendments of Fe and/or P (Supplementary Fig. S3), together
420 implying the overall phytoplankton community across entire area was N-limited and the
421 upper waters were favorable for N₂ fixation. However, the rates and *nifH* gene
422 abundances were much higher in the northeast region of our study area than in the NSCS
423 basin (Fig. 3). Rates at stations SK1 and WP were comparable to those recently reported
424 in this region (~450 μmol N m⁻² d⁻¹) measured using the same ¹⁵N₂ gas dissolution
425 method (Lu et al., 2019; Wen et al., 2022). Although relatively low rates were measured
426 at the Kuroshio Current station (K1) compared with previous observations (e.g., Wen et
427 al., 2022), high *nifH* gene abundance was nevertheless observed at this site (Fig. 3 and
428 Supplementary Table S3). Therefore, our observations provide increasing evidence for
429 this western (sub)tropical North Pacific boundary region containing important “hot spots”
430 of N₂ fixation (Shiozaki et al., 2010; Shiozaki et al., 2015a; Wen et al., 2022). However,
431 the elevated total *nifH* concentration in the western boundary of the North Pacific during
432 our study was largely attributed to an increased *nifH* abundance of unicellular diazotrophs
433 (UCYN-A and B, Fig. 3), but not *Trichodesmium* as previously reported (Chen et al.,

434 2003; Chen et al., 2008; Chen et al., 2014; Shiozaki et al., 2014a). Instead, we found that
435 *Trichodesmium nifH* gene was most abundant at stations (S3 and S4) close to the western
436 edge of the Luzon Strait (Fig. 3 and Supplementary Table S3), where Kuroshio intrusion
437 water has been hypothesized to introduce *Trichodesmium* into a favorable biogeographic
438 regime (Lu et al., 2019). Either this region is spatially and/or temporally heterogeneous
439 with respect to the presence of unicellular versus *Trichodesmium* diazotrophs, or the
440 environmental changes have led to a shift in diazotroph community structure (Gruber,
441 2011; Hutchins and Fu, 2017).

442

443 Depth-integrated N₂ fixation rate and *nifH* gene abundance were not correlated with sea
444 surface temperature (SST), but a significant positive correlation was found between
445 nitracline depth and total *nifH* gene abundance (Pearson $r = 0.74$, $p = 0.037$,
446 Supplementary Table S2). This was suggestive of subsurface N supply into the euphotic
447 zone, which is inversely related to nitracline depth, potentially being important in
448 regulating diazotroph abundance in our study area, with lower N supply leading to
449 enhanced diazotroph abundances (Chen et al., 2003; Shiozaki et al., 2014b). The presence
450 of diazotrophs in the ocean will be a function of how well they can compete with non-
451 diazotrophic phytoplankton for limiting resources (e.g., Fe and P) under grazing pressure
452 (Ward et al., 2013; Dutkiewicz et al., 2014; Landolfi et al., 2021). Accordingly, because
453 of the growth characteristics of diazotrophs in comparison to non-diazotrophs, in

454 particular their lack of requirement for pre-fixed N, but higher requirement for Fe and P,
455 the relative supply rates of N, Fe and P are highly important in dictating where
456 diazotrophs can succeed (Ward et al., 2013). Aligning with earlier global model
457 predictions (Ward et al., 2013), and investigations in the (sub)tropical Atlantic (Schlosser
458 et al., 2014), Wen et al. (2022) recently found that the Fe:N supply ratio (including
459 subsurface and aerosol N and Fe supplies) was a robust predictor of diazotroph standing
460 stock across the broader western North Pacific, including our study region.

461

462 By carrying out bioassay incubations, we observed that N₂ fixation rates in the NSCS
463 basin were either (i) ‘simultaneously co-limited’ by Fe and P (identified at station S1),
464 which represents a state where two, non-substitutable nutrients (in this case, Fe and P)
465 have been drawn down to equally limiting levels (Sperfeld et al., 2016), or (ii)
466 ‘independently co-limited’ (stations SEATS₂₀₁₆ and S3), which represents a state where
467 the resources are substitutable at biochemical (Saito et al., 2008), or community levels
468 (Arrigo, 2005). Previous studies reported relatively low surface Fe concentrations in the
469 NSCS basin (0.2-0.3 nM; Wu et al., 2003; Wen et al., 2022), although Fe supply rates to
470 this region are likely elevated via riverine, sedimental and aerosol inputs (Duce et al.,
471 1991; Jickells et al., 2005; Zhang et al., 2019). Wu et al (2003) hypothesized that the low
472 Fe concentrations were due to a lack of Fe-binding organic ligands, which was
473 subsequently restricting the growth of diazotrophs. We suggest that this may also be

474 attributed to the rapid consumption of Fe (as well as P) by the faster-growing non-
475 diazotrophs under elevated N supply (due to shallower nitraclines, alongside riverine and
476 aerosol inputs). Thus we hypothesize that with the lower Fe:N supply ratio, diazotrophs
477 in this region were outcompeted by non-diazotrophic phytoplankton and co-limited by
478 both Fe and P (Fig. 4). These results add to increasing evidence for the potentially
479 widespread Fe-P colimitation of N₂ fixation under elevated Fe supply (Mills et al., 2004;
480 Snow et al., 2015; Cerdan-Garcia et al., 2022).

481

482 The measured contributions of individual diazotrophs to total *nifH* concentration in
483 response to nutrient supply suggested that simultaneous Fe-P co-limitation of N₂ fixation
484 rates at station S1 was via regulation of *Trichodesmium*, which only responded to Fe+P
485 addition (Fig. 5). The *nifH* responses also suggested that independent Fe-P co-limitation
486 of N₂ fixation rates at sites SEATS₂₀₁₆ and S3 was not operating at the community level
487 (i.e., one diazotroph type limited by Fe and the other by P; Arrigo, 2005), as different
488 qPCR-based diazotroph community structure responses to either Fe or P addition were
489 not observed (Fig. 5). We suggest three possible causes for this observation: (i) co-
490 limitation was at the biochemical rather than community level (i.e., either Fe or P could
491 enhance the rates of processes ultimately driving elevated N₂ fixation; Saito et al., 2008).
492 For instance, in addition to serving as a cofactor in nitrogenase, Fe is also a cofactor in
493 alkaline phosphatases (Rodriguez et al., 2014; Yong et al., 2014). Thus, the addition of Fe

494 may allow for enhanced utilization of dissolved organic P (DOP) under depleted DIP
495 (Browning et al., 2017); (ii) other diazotrophs, which were not analyzed by the qPCR
496 assay, may be responsible for the enhanced N₂ fixation rates after nutrient additions; or
497 (iii) community co-limitation of N₂ fixation rates for the measured groups was occurring,
498 but, unlike the simultaneous co-limitation scenario at station S1, experimental durations
499 were too short for this to be reflected in diazotroph biomass changes. Surprisingly,
500 stations with independent co-limitation of N₂ fixation rates by Fe and P (SEATS₂₀₁₆ and
501 S3) were not additive (i.e., increases in N₂ fixation rates in Fe+P treatments were not
502 larger than Fe and P alone; Sperfeld et al., 2016). Although the available data do not
503 allow us to provide a concrete reason for this, the absence of this additive response may
504 reflect one or a combination of (i) addition of Fe or P leading to the depletion of another
505 secondary limitation nutrient (e.g., Ni), (ii) overall light levels setting an upper limit of N₂
506 fixation rates, which prevented further enhancements after nutrient additions, or (iii)
507 grazer regulation of diazotroph biomass accumulation.

508

509 In contrast to the more central NSCS, the deeper nitraclines in the western boundary of
510 the North Pacific appeared more favorable for N₂ fixation (Fig. 3 and Table 1). P
511 limitation of N₂ fixation at these sites implied that Fe supply (e.g., via aerosols)
512 stimulated diazotroph growth (Fig. 3; Wen et al., 2022) and subsequently drawdown P to
513 limiting levels (Table 1, Figs 4 and 5, Hashihama et al., 2009; Ward et al., 2013; Wen et

514 al., 2022). Additional Fe inputs other than aerosol deposition are also potentially
515 important in supporting the elevated N₂ fixation in the Luzon Strait. At station SK2, much
516 higher surface particulate Fe concentrations (both intracellular and total forms) were
517 observed (Supplementary Table S4), implying supplementary Fe inputs potentially
518 sourced from the adjacent islands and the surrounding shallow sub-surface bathymetry
519 (Shiozaki et al., 2014a; Shiozaki et al., 2015a).

520

521 In addition to the Fe:N supply ratio regulating the total *nifH* gene abundance and activity
522 (Wen et al., 2022), we also further hypothesize that overall Fe supply rates might be an
523 important factor in determining the diazotroph community structure in our study area
524 (Church et al., 2008; Langlois et al., 2008; Shiozaki et al., 2017). Specifically, the depth-
525 integrated diazotroph compositions of the six phylotypes switched from being co-
526 dominated by *Trichodesmium* and other diazotrophs in the central NSCS (SEATS, S1 and
527 S2), *Trichodesmium*-dominated in the more northern NSCS (S3 and S4), and finally
528 dominated by UCYN-B in the western boundary of the North Pacific (Fig. 3 and
529 Supplementary Table S3). Elevated Fe supply in the NSCS, particularly around the
530 islands and shallow bathymetry of the Luzon Strait, might create a more favorable
531 condition for *Trichodesmium* (Fig. 3 and Supplementary Table S3), consistent with
532 elevated Fe demands of this species (Kustka et al., 2003; Kupper et al., 2008; Sohm et al.,
533 2011), as well as its ability to use particulate Fe forms (Rubin et al., 2011), and in line

534 with the elevated contribution of this species found in other regions with enhanced Fe
535 supply (e.g., the tropical North Atlantic and western South Pacific; Sañudo-Wilhelmy et
536 al., 2001; Sohm et al., 2011; Bonnet et al. 2018; Stenegren et al., 2018). In fact, Fe
537 stimulation of *Trichodesmium nifH* abundance was observed in the experiment conducted
538 at station S4 (Supplementary Fig. S2). At station S3, however, this was only observed for
539 N₂ fixation rates but not *Trichodesmium nifH* abundance (Supplementary Fig. S2). We
540 suggest this could reflect a variable decoupling of N₂ fixation rates and diazotroph
541 abundance, depending on other environmental and/or ecological conditions. Conversely,
542 unicellular species may be more competitive than *Trichodesmium* in regions with lower
543 Fe supply rates (Fig. 3). In addition to having a higher surface to volume ratio that favors
544 Fe uptake (Hudson and Morel 1990; Jacq et al., 2014), UCYN-B species such as
545 *Crocospaera* have been reported to employ a repertoire of Fe-conservation strategies,
546 e.g., daily synthesis and breakdown of metalloproteins to recycle Fe between the
547 photosynthetic and N₂ fixation metalloenzymes and increased expression of flavodoxin at
548 night even under Fe-replete conditions (Saito et al., 2011). These potentially explain why
549 UCYN-B was less Fe-limited in the NSCS basin (stations SEATS₂₀₁₆ and S1; Fig. 5 and
550 Supplementary Fig. S2) and dominates the diazotroph community on the western Pacific
551 side of the Luzon Strait (Fig. 3; Chen et al., 2019; Wen et al., 2022). Future work with
552 paired measurements of Fe supply rates to surface waters and diazotroph community
553 structure throughout the region would allow for more robust testing of this hypothesis.

554

555 **5 Conclusions**

556 Observations and experiments conducted in the NSCS and the western boundary of the
557 North Pacific demonstrated that in the more central NSCS, Fe and P were co-limiting the
558 lower overall observed N₂ fixation rates, whereas P was limiting the higher rates on the
559 western Pacific side of the Luzon Strait. This matched the expectation of higher Fe:N
560 supply ratios in the western Pacific generating a more favorable niche for diazotrophs,
561 leading to a drawdown of *P. Trichodesmium* and UCYN-B were the most dominant *nifH*
562 phylotypes in the incubation waters and both dominated the responses of the total *nifH*
563 gene after nutrient amendments. In general, nutrient addition had a relatively restricted
564 impact on qPCR-based diazotroph community structure apart from on UCYN-B, which
565 showed increased contribution in the diazotroph community following P addition at sites
566 where N₂ fixation rates were P-limited. We hypothesize that overall switches in
567 diazotroph community structure from *Trichodesmium*-dominated in the NSCS to single-
568 celled UCYNA/B was related to declines in overall Fe supply rates and the different
569 physiological strategies of these diazotrophs to obtain and use Fe. Future research that
570 more accurately constrains nutrient supply rates to these different regions would be
571 beneficial for further resolving this hypothesis.

572 *Data availability.* All data needed to evaluate the conclusions in the paper are present in
573 the paper and/or the Supplementary Materials. Additional data associated with the paper
574 are available from the corresponding authors upon request.

575

576 *Author contributions.* D.S., H.H., and Z.W. designed the research. Z.W., R.D., W.W.,
577 W.L., X.H., W.L., and L.W. performed the experiments. Z.W., D.S., H.H., T.J.B., X.L.,
578 and Z.C. analyzed the data. Z.W., T.J.B., H.H., and D.S. wrote the manuscript. All authors
579 discussed the results and commented and edited the manuscript.

580

581 *Competing interests.* The authors declare that they have no conflict of interest.

582

583 *Acknowledgements.* The authors acknowledge the captains and crew of the R/V
584 *Dongfanghong 2* and R/V *Tan Kah Kee* for the help during the cruises. This work was
585 supported by the National Science Foundation of China (41890802, 42076149,
586 41925026, 42106041, and 41721005), the “111” Project (BP0719030), and the
587 XPLOER Prize from the Tencent Foundation to D. Shi.

588 **References**

- 589 Arrigo, K. R.: Marine microorganisms and global nutrient cycles, *Nature*, 437, 349-355,
590 10.1038/nature04158, 2005.
- 591 Berman-Frank, I., Cullen, J. T., Shaked, Y., Sherrell, R. M., and Falkowski, P.: Iron
592 availability, cellular iron quotas, and nitrogen fixation in *Trichodesmium*, *Limnol.*
593 *Oceanogr.*, 46, 1249-1260, 10.4319/lo.2001.46.6.1249, 2001.
- 594 Bonnet, S., Baklouti, M., Gimenez, A., Berthelot, H., and Berman-Frank, I.:
595 Biogeochemical and biological impacts of diazotroph blooms in a low-nutrient,
596 low-chlorophyll ecosystem: synthesis from the VAHINE mesocosm experiment
597 (New Caledonia), *Biogeosciences*, 13, 4461-4479, 10.5194/bg-13-4461-2016, 2016.
- 598 Bonnet, S., Caffin, M., Berthelot, H., Grosso, O., Benavides, M., Helias-Nunige, S.,
599 Guieu, C., Stenegren, M., and Foster, R. A.: In-depth characterization of diazotroph
600 activity across the Western Tropical South Pacific hot spot of N₂ fixation
601 (OUTPACE cruise), *Biogeosciences*, 15, 4215-4232, 10.5194/bg-15-4215-2018,
602 2018.
- 603 Boström, K. H., Simu, K., Hagström, Å., and Riemann, L.: Optimization of DNA
604 extraction for quantitative marine bacterioplankton community analysis, *Limnol.*
605 *Oceanogr.-Methods*, 2, 365-373, 10.4319/lom.2004.2.365, 2004.
- 606 Böttjer, D., Dore, J. E., Karl, D. M., Letelier, R. M., Mahaffey, C., Wilson, S. T., Zehr, J.
607 P., and Church, M. J.: Temporal variability of nitrogen fixation and particulate

608 nitrogen export at Station ALOHA, *Limnol. Oceanogr.*, 62, 200-216,
609 10.1002/lno.10386, 2016.

610 Browning, T. J., Achterberg, E. P., Yong, J. C., Rapp, I., Utermann, C., Engel, A., and
611 Moore, C. M.: Iron limitation of microbial phosphorus acquisition in the tropical
612 North Atlantic, *Limnol. Oceanogr. Lett.*, 8, 15465, 10.1038/ncomms15465, 2017.

613 Cerdan-Garcia, E., Baylay, A., Polyviou, D., Woodward, E. M. S., Wrightson, L.,
614 Mahaffey, C., Lohan, M. C., Moore, C. M., Bibby, T. S., and Robidart, J. C.:
615 Transcriptional responses of *Trichodesmium* to natural inverse gradients of Fe and P
616 availability, *Isme J*, 16, 1055-1064, 10.1038/s41396-021-01151-1, 2022.

617 Chen, M., Lu, Y., Jiao, N., Tian, J., Kao, S. J., and Zhang, Y.: Biogeographic drivers of
618 diazotrophs in the western Pacific Ocean, *Limnol. Oceanogr.*, 64, 1403-1421,
619 10.1002/lno.11123, 2019.

620 Chen, Y. L. L., Chen, H. Y., and Lin, Y. H.: Distribution and downward flux of
621 *Trichodesmium* in the South China Sea as influenced by the transport from the
622 Kuroshio Current, *Mar. Ecol. Prog. Ser.*, 259, 47-57, 10.3354/meps259047, 2003.

623 Chen, Y. L. L., Chen, H. Y., Tuo, S. H., and Ohki, K.: Seasonal dynamics of new
624 production from *Trichodesmium* N₂ fixation and nitrate uptake in the upstream
625 Kuroshio and South China Sea basin, *Limnol. Oceanogr.*, 53, 1705-1721,
626 10.4319/lo.2008.53.5.1705, 2008.

627 Chen, Y. L. L., Chen, H. Y., Lin, Y. H., Yong, T. C., Taniuchi, Y., and Tuo, S. H.: The

628 relative contributions of unicellular and filamentous diazotrophs to N₂ fixation in
629 the South China Sea and the upstream Kuroshio, Deep Sea Research Part I, 85, 56-
630 71, 10.1016/j.dsr.2013.11.006, 2014.

631 Church, M. J., Björkman, K., and Karl, D.: Regional distributions of nitrogen-fixing
632 bacteria in the Pacific Ocean, Limnol. Oceanogr., 53, 63-77, 2008.

633 Church, M. J., Jenkins, B. D., Karl, D. M., and Zehr, J. P.: Vertical distributions of
634 nitrogen fixing phylotypes at Stn ALOHA in the oligotrophic North Pacific Ocean,
635 Aquat. Microb. Ecol., 38, 3-14, 10.3354/ame038003 2005a.

636 Church, M. J., Short, C. M., Jenkins, B. D., Karl, D. M., and Zehr, J. P.: Temporal
637 patterns of nitrogenase gene (*nifH*) expression in the oligotrophic North Pacific
638 Ocean, Appl. Environ. Microbiol., 71, 5362-5370, 10.1128/AEM.71.9.5362-
639 5370.2005, 2005b.

640 Dekaezemacker, J., Bonnet, S., Grosso, O., Moutin, T., Bressac, M., and Capone, D. G.:
641 Evidence of active dinitrogen fixation in surface waters of the eastern tropical
642 South Pacific during El Niño and La Niña events and evaluation of its potential
643 nutrient controls, Global Biogeochem. Cycles, 27, 768-779, 10.1002/gbc.20063,
644 2013.

645 Du, C., Liu, Z., Dai, M., Kao, S. J., Cao, Z., Zhang, Y., Huang, T., Wang, L., and Li, Y.:
646 Impact of the Kuroshio intrusion on the nutrient inventory in the upper northern
647 South China Sea: Insights from an isopycnal mixing model, Biogeosciences, 10,

648 6419-6432, 10.5194/bg-10-6419-2013, 2013.

649 Duce, R. A., Liss, P. S., Merrill, J. T., Atlas, E. L., Buat-Menard, P., Hicks, B. B., Miller,
650 J. M., Prospero, J. M., Arimoto, R., Church, T. M., Ellis, W., Galloway, J. N.,
651 Hansen, L., Jickells, T. D., Knap, A. H., Reinhardt, K. H., Schneider, B., Soudine,
652 A., Tokos, J. J., Tsunogai, S., Wollast, R., and Zhou, M.: The atmospheric input of
653 trace species to the world ocean, *Global Biogeochem. Cycles*, 5, 193-259,
654 10.1029/91gb01778, 1991.

655 Dutkiewicz, S., Ward, B. A., Scott, J., and Follows, M. J.: Understanding predicted shifts
656 in diazotroph biogeography using resource competition theory, *Biogeosciences*, 11,
657 5445-5461, 10.5194/bg-11-5445-2014, 2014.

658 Farnelid, H., Turk-Kubo, K., Muñoz-Marín, M. C., and Zehr, J. P.: New insights into the
659 ecology of the globally significant uncultured nitrogen-fixing symbiont UCYN-A,
660 *Aquat. Microb. Ecol.*, 77, 125-138, 10.3354/ame01794, 2016.

661 Göran, E. and Cooper, S. D.: Scale effects and extrapolation in ecological experiments,
662 *Adv. Ecol. Res.*, 33, 161-213, 10.1016/S0065-2504(03)33011-9, 2003.

663 Grabowski, M. N. W., Church, M. J., and Karl, D. M.: Nitrogen fixation rates and
664 controls at Stn ALOHA, *Aquat. Microb. Ecol.*, 52, 175-183, 10.3354/ame01209,
665 2008.

666 Gruber, N.: Warming up, turning sour, losing breath: ocean biogeochemistry under global
667 change, *Philos T R Soc A*, 369, 1980-1996, 10.1098/rsta.2011.0003, 2011.

668 Gruber, N. and Galloway, J. N.: An Earth-system perspective of the global nitrogen cycle,
669 Nature, 451, 293-296, 10.1038/nature06592, 2008.

670 Guo, L., Xiu, P., Chai, F., Xue, H. J., Wang, D. X., and Sun, J.: Enhanced chlorophyll
671 concentrations induced by Kuroshio intrusion fronts in the northern South China
672 Sea, Geophys. Res. Lett., 44, 11565-11572, 10.1002/2017GL075336, 2017.

673 Hama, T., Miyazaki, T., Ogawa, Y., Iwakuma, T., Takahashi, M., Otsuki, A., and
674 Ichimura, S.: Measurement of photosynthetic production of a marine phytoplankton
675 population using a stable ^{13}C isotope., Mar. Biol., 73, 31-36, 10.1007/BF00396282,
676 1983.

677 Hashihama, F., Furuya, K., Kitajima, S., Takeda, S., Takemura, T., and Kanda, J.: Macro-
678 scale exhaustion of surface phosphate by dinitrogen fixation in the western North
679 Pacific, Geophys. Res. Lett., 36, L03610, 10.1029/2008gl036866, 2009.

680 Huang, Y., Laws, E. A., Chen, B., and Huang, B.: Stimulation of heterotrophic and
681 autotrophic metabolism in the mixing zone of the Kuroshio Current and northern
682 South China Sea: Implications for export production, J Geophys Res-
683 Biogeosciences, 124, 2645-2661, 10.1029/2018jg004833, 2019.

684 Hudson, R. J. M. and Morel, F. M. M.: Iron transport in marine-phytoplankton - kinetics
685 of cellular and medium coordination reactions, Limnol. Oceanogr., 35, 1002-1020,
686 10.4319/lo.1990.35.5.1002, 1990.

687 Hutchins, D. A. and Fu, F.: Microorganisms and ocean global change, Nat. Microbiol., 2,

688 17058, 10.1038/nmicrobiol.2017.58, 2017.

689 Jacq, V., Ridame, C., L'Helguen, S., Kaczmar, F., and Saliot, A.: Response of the
690 unicellular diazotrophic cyanobacterium *Crocospaera watsonii* to iron limitation,
691 PLoS One, 9, e86749, 10.1371/journal.pone.0086749, 2014.

692 Jickells, T. D., An, Z. S., Andersen, K. K., Baker, A. R., Bergametti, G., Brooks, N., Cao,
693 J. J., Boyd, P. W., Duce, R. A., Hunter, K. A., Kawahata, H., Kubilay, N., laRoche,
694 J., Liss, P. S., Mahowald, N., Prospero, J. M., Ridgwell, A. J., Tegen, I., and Torres,
695 R.: Global iron connections between desert dust, ocean biogeochemistry, and
696 climate, Science, 308, 67-71, 10.1126/science.1105959, 2005.

697 Karlusich, J. J. P., Pelletier, E., Lombard, F., Carsique, M., Dvorak, E., Colin, S., Picheral,
698 M., Cornejo-Castillo, F. M., Acinas, S. G., Pepperkok, R., Karsenti, E., de Vargas,
699 C., Wincker, P., Bowler, C., Foster, R. A.: Global distribution patterns of marine
700 nitrogen-fixers by imaging and molecular methods, Nat. Commun., 12,
701 10.1038/s41467-021-24299-y, 2021.

702 Krupke, A., Mohr, W., LaRoche, J., Fuchs, B. M., Amann, R. I., and Kuypers, M. M.: The
703 effect of nutrients on carbon and nitrogen fixation by the UCYN-A-haptophyte
704 symbiosis, Isme J, 9, 1635-1647, 10.1038/ismej.2014.253, 2015.

705 Kustka, A., Sañudo-Wilhelmy, S., Carpenter, E. J., Capone, D. G., and Raven, J. A.: A
706 revised estimate of the iron use efficiency of nitrogen fixation, with special
707 reference to the marine cyanobacterium *Trichodesmium* spp. (cyanophyta), J.

708 Phycol., 39, 12-25, 10.1046/j.1529-8817.2003.01156.x, 2003.

709 Kupper, H., Setlik, I., Seibert, S., Prasil, O., Setlikova, E., Strittmatter, M., Levitan, O.,
710 Lohscheider, J., Adamska, I., and Berman-Frank, I.: Iron limitation in the marine
711 cyanobacterium *Trichodesmium* reveals new insights into regulation of
712 photosynthesis and nitrogen fixation, *New Phytol.*, 179, 784-798, 10.1111/j.1469-
713 8137.2008.02497.x, 2008.

714 Landolfi, A., Prowe, A. E. F., Pahlow, M., Somes, C. J., Chien, C. T., Schartau, M.,
715 Koeve, W., and Oschlies, A.: Can top-down controls expand the ecological niche of
716 marine N₂ fixers?, *Front Microbiol*, 12, 690200, 10.3389/fmicb.2021.690200, 2021.

717 Langlois, R. J., Hummer, D., and LaRoche, J.: Abundances and distributions of the
718 dominant *nifH* phylotypes in the Northern Atlantic Ocean, *Appl. Environ.*
719 *Microbiol.*, 74, 1922-1931, 10.1128/AEM.01720-07, 2008.

720 Langlois, R. J., Mills, M. M., Ridame, C., Croot, P., and LaRoche, J.: Diazotrophic
721 bacteria respond to Saharan dust additions, *Mar. Ecol. Prog. Ser.*, 470, 1-14,
722 10.3354/meps10109, 2012.

723 Le Borgne, R., Barber, R. T., Delcroix, T., Inoue, H. Y., Mackey, D. J., and Rodier, M.:
724 Pacific warm pool and divergence: Temporal and zonal variations on the equator
725 and their effects on the biological pump, *Deep Sea Research Part II*, 49, 2471-2512,
726 10.1016/S0967-0645(02)00045-0, 2002.

727 Li, W., Sunda, W. G., Lin, W., Hong, H., and Shi, D.: The effect of cell size on cellular Zn

728 and Cd and Zn-Cd-CO₂ colimitation of growth rate in marine diatoms, *Limnol.*
729 *Oceanogr.*, 65, 2896-2911, 10.1002/lno.11561, 2020.

730 Li, X., Wu, K., Gu, S., Jiang, P., Li, H., Liu, Z., and Dai, M.: Enhanced biodegradation of
731 dissolved organic carbon in the western boundary Kuroshio Current when intruded
732 to the marginal South China Sea, *J Geophys Res-Oceans*, 126, e2021JC017585,
733 10.1029/2021jc017585, 2021.

734 Lu, Y., Wen, Z., Shi, D., Lin, W., Bonnet, S., Dai, M., and Kao, S. J.: Biogeography of N₂
735 fixation influenced by the western boundary current intrusion in the South China
736 Sea, *J Geophys Res-Oceans*, 124, 6983-6996, 10.1029/2018jc014781, 2019.

737 Ma, J., Yuan, D. X., Liang, Y., and Dai, M. H.: A modified analytical method for the
738 shipboard determination of nanomolar concentrations of orthophosphate in
739 seawater, *J Oceanogr*, 64, 443-449, 2008.

740 Mohr, W., Großkopf, T., Wallace, D. W., and LaRoche, J.: Methodological
741 underestimation of oceanic nitrogen fixation rates, *PLoS One*, 5, e12583,
742 10.1371/journal.pone.0012583.g001, 2010.

743 Moisander, P. H., Beinart, R. A., Voss, M., and Zehr, J. P.: Diversity and abundance of
744 diazotrophic microorganisms in the South China Sea during intermonsoon, *Isme J*,
745 2, 954-967, 10.1038/ismej.2008.51, 2008.

746 Moisander, P. H., Zhang, R., Boyle, E. A., Hewson, I., Montoya, J. P., and Zehr, J. P.:
747 Analogous nutrient limitations in unicellular diazotrophs and *Prochlorococcus* in

748 the South Pacific Ocean, *Isme J*, 6, 733-744, 10.1038/ismej.2011.152, 2012.

749 Montoya, J. P., Voss, M., Kähler, P., and Capone, D. G.: A simple, high-precision, high-
750 sensitivity tracer assay for N₂ fixation, *Appl. Environ. Microbiol.*, 62, 986-993,
751 10.1128/AEM.62.3.986-993.1996, 1996.

752 Needoba, J. A., Foster, R. A., Sakamoto, C., Zehr, J. P., and Johnson, K. S.: Nitrogen
753 fixation by unicellular diazotrophic cyanobacteria in the temperate oligotrophic
754 North Pacific Ocean, *Limnol. Oceanogr.*, 54, 1317–1327,
755 10.4319/lo.2007.52.4.1317, 2007.

756 Rodriguez, F., Lillington, J., Johnson, S., Timmel, C. R., Lea, S. M., and Berks, B. C.:
757 Crystal structure of the bacillus subtilis phosphodiesterase PhoD reveals an iron and
758 calcium-containing active site, *J. Biol. Chem.*, 289, 30889-30899,
759 10.1074/jbc.M114.604892, 2014.

760 Rubin, M., Berman-Frank, I., and Shaked, Y.: Dust- and mineral-iron utilization by the
761 marine dinitrogen-fixer *Trichodesmium*, *Nat Geosci*, 4, 529-534,
762 10.1038/ngeo1181, 2011.

763 Saito, M. A., Goepfert, T. J., and Ritt, J. T.: Some thoughts on the concept of colimitation:
764 Three definitions and the importance of bioavailability, *Limnol. Oceanogr.*, 53, 276-
765 290, 10.4319/lo.2008.53.1.0276, 2008.

766 Saito, M. A., Bertrand, E. M., Dutkiewicz, S., Bulygin, V. V., Moran, D. M., Monteiro, F.
767 M., Follows, M. J., Valois, F. W., and Waterbury, J. B.: Iron conservation by

768 reduction of metalloenzyme inventories in the marine diazotroph *Crocospaera*
769 *watsonii*, Proc. Natl. Acad. Sci. U.S.A., 108, 2184-2189,
770 10.1073/pnas.1006943108, 2011.

771 Sañudo-Wilhelmy, S. A., Kustka, A. B., Gobler, C. J., Hutchins, D. A., Yang, M., Lwiza,
772 K., Burns, J. A., Capone, D. G., Ravenk, J. A., and Carpenter, E. J.: Phosphorus
773 limitation of nitrogen fixation by *Trichodesmium* in the central Atlantic Ocean,
774 Nature, 411, 66-69, 10.1038/35075041, 2001.

775 Sargent, E. C., Hitchcock, A., Johansson, S. A., Langlois, R., Moore, C. M., LaRoche, J.,
776 Poulton, A. J., and Bibby, T. S.: Evidence for polyploidy in the globally important
777 diazotroph *Trichodesmium*, FEMS Microbiol. Lett., 363, 10.1093/femsle/fnw244,
778 2016.

779 Schlosser, C., Klar, J. K., Wake, B. D., Snow, J. T., Honey, D. J., Woodward, E. M. S.,
780 Lohan, M. C., Achterberg, E. P., and Moore, C. M.: Seasonal ITCZ migration
781 dynamically controls the location of the (sub)tropical Atlantic biogeochemical
782 divide, Proc. Natl. Acad. Sci. U.S.A., 111, 1438-1442, 10.1073/pnas.1318670111,
783 2014.

784 Shiozaki, T., Kodama, T., and Furuya, K.: Large-scale impact of the island mass effect
785 through nitrogen fixation in the western South Pacific Ocean, Geophys. Res. Lett.,
786 41, 2907-2913, 10.1002/2014GL059835 2014a.

787 Shiozaki, T., Nagata, T., Ijichi, M., and Furuya, K.: Nitrogen fixation and the diazotroph

788 community in the temperate coastal region of the northwestern North Pacific,
789 Biogeosciences, 12, 4751-4764, 10.5194/bg-12-4751-2015, 2015a.

790 Shiozaki, T., Chen, Y. L. L., Lin, Y. H., Taniuchi, Y., Sheu, D. S., Furuya, K., and Chen,
791 H. Y.: Seasonal variations of unicellular diazotroph groups A and B, and
792 *Trichodesmium* in the northern South China Sea and neighboring upstream
793 Kuroshio Current, Cont. Shelf Res., 80, 20-31, 10.1016/j.csr.2014.02.015, 2014b.

794 Shiozaki, T., Furuya, K., Kodama, T., Kitajima, S., Takeda, S., Takemura, T., and Kanda,
795 J.: New estimation of N₂ fixation in the western and central Pacific Ocean and its
796 marginal seas, Global Biogeochem. Cycles, 24, GB1015, 10.1029/2009gb003620,
797 2010.

798 Shiozaki, T., Takeda, S., Itoh, S., Kodama, T., Liu, X., Hashihama, F., and Furuya, K.:
799 Why is *Trichodesmium* abundant in the Kuroshio?, Biogeosciences, 12, 6931-6943,
800 10.5194/bg-12-6931-2015, 2015b.

801 Shiozaki, T., Bombar, D., Riemann, L., Hashihama, F., Takeda, S., Yamaguchi, T.,
802 Ehama, M., Hamasaki, K., and Furuya, K.: Basin scale variability of active
803 diazotrophs and nitrogen fixation in the North Pacific, from the tropics to the
804 subarctic Bering Sea, Global Biogeochem. Cycles, 31, 996-1009
805 10.1002/2017gb005681, 2017.

806 Snow, J. T., Schlosser, C., Woodward, E. M., Mills, M., Achterberg, E. P., Mahaffey, C.,
807 Bibby, T. S., and Moore, C. M.: Environmental controls on the biogeography of

808 diazotrophy and *Trichodesmium* in the Atlantic Ocean, *Global Biogeochem. Cycles*,
809 29, 865-884, 10.1002/2015GB005090, 2015.

810 Sohm, J. A., Webb, E. A., and Capone, D. G.: Emerging patterns of marine nitrogen
811 fixation, *Nature reviews. Microbiology*, 9, 499-508, 10.1038/nrmicro2594, 2011.

812 Sperfeld, E., Raubenheimer, D., and Wacker, A.: Bridging factorial and gradient concepts
813 of resource co-limitation: Towards a general framework applied to consumers, *Ecol.*
814 *Lett.*, 19, 201-215, 10.1111/ele.12554, 2016.

815 Stenegren, M., Caputo, A., Berg, C., Bonnet, S., and Foster, R. A.: Distribution and
816 drivers of symbiotic and free-living diazotrophic cyanobacteria in the western
817 tropical South Pacific, *Biogeosciences*, 15, 1559-1578, 10.5194/bg-15-1559-2018,
818 2018.

819 Tanita, I., Shiozaki, T., Kodama, T., Hashihama, F., Sato, M., Takahashi, K., and Furuya,
820 K.: Regionally variable responses of nitrogen fixation to iron and phosphorus
821 enrichment in the Pacific Ocean, *Journal of Geophysical Research: Biogeosciences*,
822 126, e2021JG006542, 10.1029/2021jg006542, 2021.

823 Thompson, A. W., Carter, B. J., Turk-Kubo, K. A., Malfatti, F., Azam, F., and Zehr, J. P.:
824 Genetic diversity of the unicellular nitrogen-fixing cyanobacteria UCYN-A and its
825 prymnesiophyte host, *Environ. Microbiol.*, 16, 3238-3249, 10.1111/1462-
826 2920.12490, 2014.

827 Turk-Kubo, K. A., Achilles, K. M., Serros, T. R., Ochiai, M., Montoya, J. P., and Zehr, J.

828 P.: Nitrogenase (*nifH*) gene expression in diazotrophic cyanobacteria in the Tropical
829 North Atlantic in response to nutrient amendments, *Front Microbiol*, 3, 386,
830 10.3389/fmicb.2012.00386, 2012.

831 Wang, W. L., Moore, J. K., Martiny, A. C., and Primeau, F. W.: Convergent estimates of
832 marine nitrogen fixation, *Nature*, 566, 205-211, 10.1038/s41586-019-0911-2, 2019.

833 Ward, B. A., Dutkiewicz, S., Moore, C. M., and Follows, M. J.: Iron, phosphorus, and
834 nitrogen supply ratios define the biogeography of nitrogen fixation, *Limnol.*
835 *Oceanogr.*, 58, 2059-2075, 10.4319/lo.2013.58.6.2059, 2013.

836 Watkins-Brandt, K. S., Letelier, R. M., Spitz, Y. H., Church, M. J., Böttjer, D., and White,
837 A. E.: Addition of inorganic or organic phosphorus enhances nitrogen and carbon
838 fixation in the oligotrophic North Pacific, *Mar. Ecol. Prog. Ser.*, 432, 17-29,
839 10.3354/meps09147, 2011.

840 Welschmeyer, N. A.: Fluorometric analysis of chlorophyll-a in the presence of
841 chlorophyll-B and pheopigments, *Limnol. Oceanogr.*, 39, 1985-1992, 1994.

842 Wen, Z., Browning, T. J., Cai, Y., Dai, R., Zhang, R., Du, C., Jiang, R., Lin, W., Liu, X.,
843 Cao, Z., Hong, H., Dai, M., and Shi, D.: Nutrient regulation of biological nitrogen
844 fixation across the tropical western North Pacific, *Sci. Adv.*, 8, eabl7564,
845 10.1126/sciadv.abl7564, 2022.

846 White, A. E., Watkins-Brandt, K.S., and Church, M. J.: Temporal variability of
847 *Trichodesmium* spp. and diatom-diazotroph assemblages in the North Pacific

848 Subtropical Gyre, *Front. Mar. Sci.*, 5, 10.3389/fmars.2018.00027, 2018.

849 Wu, C., Fu, F. X., Sun, J., Thangaraj, S., and Pujari, L.: Nitrogen fixation by
850 *Trichodesmium* and unicellular diazotrophs in the northern South China Sea and the
851 Kuroshio in summer, *Sci Rep-Uk*, 8, 2415, 10.1038/s41598-018-20743-0, 2018.

852 Wu, J., Chung, S. W., Wen, L. S., Liu, K. K., Chen, Y. L. L., Chen, H. Y., and Karl, D.
853 M.: Dissolved inorganic phosphorus, dissolved iron, and *Trichodesmium* in the
854 oligotrophic South China Sea, *Global Biogeochem. Cycles*, 17, 1008,
855 10.1029/2002gb001924, 2003.

856 Xu, M. N., Zhang, W., Zhu, Y., Liu, L., Zheng, Z., Wan, X. H. S., Qian, W., Dai, M., Gan,
857 J., Hutchins, D. A., and Kao, S. J.: Enhanced ammonia oxidation caused by lateral
858 Kuroshio intrusion in the boundary zone of the northern South China Sea, *Geophys.*
859 *Res. Lett.*, 45, 6585-6593, 10.1029/2018gl077896, 2018.

860 Yong, S. C., Roversi, P., Lillington, J., Rodriguez, F., Krehenbrink, M., Zeldin, O. B.,
861 Garman, E. F., Lea, S. M., and Berks, B. C.: A complex iron-calcium cofactor
862 catalyzing phosphotransfer chemistry, *Science*, 345, 1170-1173,
863 10.1126/science.1254237, 2014.

864 Zehr, J. P. and Capone, D. G.: Changing perspectives in marine nitrogen fixation,
865 *Science*, 368, eaay9514, 10.1126/science.aay9514, 2020.

866 Zhang, J. Z.: Shipboard automated determination of trace concentrations of nitrite and
867 nitrate in oligotrophic water by gas-segmented continuous flow analysis with a

868 liquid waveguide capillary flow cell, Deep Sea Research Part I, 47, 1157-1171,
869 10.1016/S0967-0637(99)00085-0, 2000.

870 Zhang, R., Zhu, X., Yang, C., Ye, L., Zhang, G., Ren, J. L., Wu, Y., Liu, S. M., Zhang, J.,
871 and Zhou, M.: Distribution of dissolved iron in the Pearl River (Zhujiang) Estuary
872 and the northern continental slope of the South China Sea, Deep Sea Research Part
873 II, 167, 14-24, 10.1016/j.dsr2.2018.12.006, 2019.